Biochemical and Biophysical Research Communications 458 (2015) 369–374

Contents lists available at ScienceDirect

Biochemical and Biophysical Research Communications

journal homepage: www.elsevier.com/locate/ybbrc

Crystal structure of dehydratase component HadAB complex of mycobacterial FAS-II pathway

Rupam Biswas [a], Anirudha Dutta [a], Debajyoti Dutta [a, 1], Ditipriya Hazra [a], Deb Ranjan Banerjee [b], Amit Basak [b], Amit Kumar Das [a, *]

[a] Department of Biotechnology, Indian Institute of Technology, Kharagpur, Kharagpur 721302, India
[b] Department of Chemistry, Indian Institute of Technology, Kharagpur, Kharagpur 721302, India

ARTICLE INFO

Article history:
Received 23 January 2015
Accepted 25 January 2015
Available online 3 February 2015

Keywords:
Mycolic acid
Double hot-dog fold
Dehydratase
Mycobacterium tuberculosis

ABSTRACT

Fatty acid biosynthesis type II in mycobacteria delivers the fatty acids required for mycolic acid synthesis. The pathway employs a unique maoC like β-hydroxyacyl-ACP dehydratase HadAB or HadBC heterodimer in the third step of the elongation cycle. Here we report the crystal structure of the HadAB complex determined using a Pb-SIRAS method. Crystal structure aided with enzymatic study establishes the roles of HadA as a scaffolding component and HadB as a catalytic component together indispensable for the activity. The detailed structural analysis of HadAB in combination with MD simulation endorses the spatial orientation of the central hot-dog helix and the dynamic nature of its associated loop in regulation of substrate specificities in dehydratase/hydratase family enzymes.

1. Introduction

Mycobacterium tuberculosis shows tolerance against various drugs by developing a lipid rich outer layer in its cell wall. The lipid rich layer also plays a major role in mycobacterial pathogenesis and responsible for the bacillus persistency within the host cell. The layer is typically composed of very long chain (C_{60} toC_{90}) fatty acid derivatives of which one of the prevalent components is Mycolic acid (MA). MAs are crucial not only for the cell wall architecture but also contribute to the drug resistance by forming a selectively permeable envelope. Therefore, MA biosynthesis is an essential pathway that can be used to develop frontline anti-tuberculosis drugs.

In Mycobacteria, there are two distinct fatty acid synthesis (FAS) pathways that come in sequence, FAS-I and FAS-II [1]. FAS-I is a mammalian cytoplasmic like single enzyme with a multi-domain system that has the ability to extend fatty acids up to C_{20}–C_{26} starting from acetyl-CoA [2]. The bacterial or plant like FAS-II is a disintegrated system of the enzymes which further elongates the FAS-I products to full length fatty acids (C_{60}–C_{90}) required for MA synthesis [3]. FAS-II elongation cycle works on acyl carrier protein (ACP) tagged fatty acyl chain and starts from condensing acyl-ACP with malonyl-ACP to yield β-ketoacyl-ACP and then in second step β-ketoacyl-ACP is reduced to β-hydroxyacyl-ACP coupled with NADPH to $NADP^+$ conversion. The third step employs the elimination of a water molecule to introduce an unsaturation between C_α–C_β and the final step is a NADH dependent reduction of the C_α–C_β unsaturation. In bacteria, classically this third step of FAS-II elongation cycle is catalysed by either a (3R)-hydroxyacyl-ACP dehydratase (FabZ) or a (3R)-hydroxyacyl-ACP dehydratase/isomerase (FabA) [4]. But in mycobacteria there is no FabZ/FabA *Escherichia coli* homologue gene present; instead a conserved gene: *htdX* (*rv0241c*) and a conserved gene cluster consisting of *hadA* (*rv0635*), *hadB* (*rv0636*) and *hadC* (*rv0637*) are found. *HtdX* [5–7] is present in proximity to FabG4, a NADH dependent β-ketoacyl reductase [8] that do not participate in FAS-II. Although HtdX is a (3R)-hydroxyacyl dehydratase exact role of the enzyme in mycobacteria is remained elusive [6]. On the contrary *hadA*, *hadB* and *hadC* are essential for the third step of the FAS-II cycle [9,10]. To carry out the third dehydration step, HadB forms heterodimer either with HadA or with HadC. HadAB complex functions during the early and middle steps of FAS-II elongation cycle whereas HadBC complex participate in during the final elongation steps. The dehydratase step in Mycobacterial FAS-II is unique in the sense that it requires three different proteins whereas in plant and bacterial FAS-II pathway corresponding step is carried out by a single enzyme FabA/FabZ. Additionally, none of these proteins have

* Corresponding author. Fax: +91 3222 255303/278707.
E-mail address: amitk@hijli.iitkgp.ernet.in (A.K. Das).
[1] Current address: Department of Biochemistry, University of Alberta, 347 Medical Science Bldg., Edmonton AB T6G 2H7, Canada.

http://dx.doi.org/10.1016/j.bbrc.2015.01.119
0006-291X/

significant sequence homology with FabA/FabZ. While FabA/FabZ forms homodimer, HadABC form heterodimer and although HadA and HadC share 45% sequence identity, they share 13–15% sequence identity with their common partner HadB. In this study we report the crystal structure of mycobacterial HadAB complex and attempted to explain the unique structural features associated with these enzymes.

2. Materials and methods

2.1. Cloning overexpression and purification

For cloning *hadAB* together, the genomic portion of the chromosomal DNA of *Mycobacterium smegmatis* mc^2 155 encoding *hadA* (MSMEG_1340) and *hadB* (MSMEG_1341) together was amplified by polymerase chain reaction (PCR) with *Pfu* DNA polymerase. The primers used 5′ CGGGATCCGTGGCTCTGTCGTCGAAAATCG 3′ (forward) and 5′ CCCAAGCTTCTAGGCGAGTCGTGCG 3′ (reverse), contain *Bam*HI and *Hin*dIII site respectively (underlined). To clone only *hadB* gene, reverse primer was the same as before and the forward primer5′ CGGGATCCATGGCTCTGCGTGAGTTCAG 3′ was used containing *Bam*HI site. Both the amplified PCR products were subcloned into pQE30 vector (Qiagen) to generate an expression plasmid encoding the full-length *hadAB* as well as *hadB* with N-terminal His_6-tag. The resulting constructs pQE30:*hadAB* and pQE30:*hadB* were transformed into *E. coli* SG13009 (pREP4) cell. The positive clones were verified by DNA sequencing. The positive transformed cells harbouring *hadAB* and *hadB* with N-terminal His_6-tag were grown in Luria broth supplemented with 100 μg ml^{-1} ampicillin and 25 μg ml^{-1} kanamycin at 310 K. Cells were induced with 250 μM IPTG for HadAB and 100 μM IPTG for HadB expression when OD_{600} was reached to 0.6 and incubated further at 288 K overnight (16 h) to ensure maximum expression of the recombinant protein. For HadAB the overexpressed cells were harvested and lysed by ultrasonication in buffer A (10 mM Tris–HCl pH 8.0, 300 mM NaCl, 10 mM imidazole) containing 0.1 mM each of leupeptin, pepstatin and aprotinin, and 0.02 mM phenylmethylsulfonyl fluoride (PMSF). After centrifugation of lysate at 14 000 rev min^{-1} for 40 min, the supernatant was loaded onto Ni-Sepharose High Performance affinity matrix (GE Healthcare Biosciences). After washing the column with buffer B (10 mM Tris–HCl pH 8.0, 300 mM NaCl, 50 mM imidazole) the protein was finally eluted with buffer C (10 mM Tris–HCl pH 8.0, 300 mM NaCl, 300 mM imidazole) as heterodimeric complex. The eluted protein was subjected to size-exclusion chromatography using Superdex 75 prep-grade matrix in a 16/70C column (GE Healthcare Biosciences) with buffer D (10 mM Tris–HCl pH 8.0, 150 mM NaCl, 2 mM DTT). For HadB purification in all buffers additionally 5% glycerol was added. As confirmed by the size-exclusion chromatography HadAB was eluted as tetramer $HadA_2B_2$ (dimer of heterodimer) whereas HadB was predominantly exist as homodimer ($HadB_2$).

2.2. Enzymatic activity assay

The activities of purified HadAB and HadB were assayed by determining the hydration of crotonoyl-CoA in 50 mM HEPES pH 7.5 buffer, 50 mM NaCl and 100 nM enzyme at 25 °C. Crotonoyl-CoA concentration was varied from 0 to 100 μM. In the reaction crotonoyl-CoA was converted into β-hydroxybutyryl-CoA and the decrease of absorbance was monitored at 263 nm.

2.3. Crystallization, data collection and structure determination

The purified HadAB protein was concentrated to 18 mg/ml and used for crystallization. Suitable crystals for diffraction experiment were obtained in 1.75 M $(NH_4)_2SO_4$, 0.1 M HEPES pH 6.8, 2% PEG 400. Prior to data collection, the crystals were quick-soaked in mother solution additionally containing 15% (v/v) glycerol and flash-cooled in a nitrogen stream at 93 K. All the diffraction data were collected in in-house X-ray diffractometer containing Cu K_α X-rays generated by a Rigaku Micromax HF007 rotating anode generator and equipped with Rigaku R-AXIS IV^{++} image-plate detector. HadAB crystals were soaked in 20 mM tri-methyl lead acetate (TMLA) for 3 h. Diffraction data were processed by using XDS [11]. Two lead sites in HadAB were located with SHELX [12] and phase was obtained by using Sharp [13]. Automated model building was done by Buccaneer [14]. Final model building and refinement was performed by coot and refmac5 [15,16]. The X-ray diffraction and structure refinement statistics are summarised in Table 1. The final structure has been deposited in PDB under the accession code 4RV2. PDBePISA was used for interface analysis in tetrameric assembly as well as in heterodimeric assembly. For structural alignment, active site analysis and image preparation PyMol was used (http://www.pymol.org).

2.4. Molecular dynamics simulation

Molecular dynamics simulation was done using GROMACS 4.5.5 software package with OPLS/AA force field [17,18]. The protein structure was solvated with SPC water models in a cubic box. The minimal distance between the box boundary and the protein atoms was kept 10 Å. The negative charges (−11) of the system were neutralized by addition of counter ions (11 Na^+) into the system. The solvated system was first energy minimized till the maximum force reaches 100 kJ mol^{-1} nm^{-1}. The system was then equilibrated

Table 1
Data collection and refinement parameters.

	Native	Pb derivative
Wavelength (Å)	1.5418	
Space group	P 4 3 2	
Cell parameter (Å, °)		
a = b = c	132.36	132.68
α = β = γ	90	90
Resolution range (Å)	19.73–2.70 (2.86–2.70)	19.56–3.00 (3.18–3.00)
No. of reflections (Total)	476766 (68257)	352523 (50842)
No. of reflections (unique)	11408 (1617)	8474 (1212)
Completeness (%)	99.5 (99.8)	99.6 (99.7)
R_{merge} (%)[a]	15.8 (72.8)	14.5 (68.2)
CC(1/2)	99.9 (96.9)	99.9 (95.4)
I/σ(I)	36.2 (7.38)	34.9 (8.1)
Redundancy	41.8 (42.2)	41.6 (41.9)
No. of Pb sites		2
R_{cullis} (iso)		0.936
R_{cullis} (ano)		0.948
Phasing power iso (acentric)		0.549
Phasing power ano (acentric)		0.462
Wilson B-factor ($Å^2$)	36.0	
R_{work}[b]/R_{free}[c]	21.6/28.6	
R.m.s deviation		
Bond lengths (Å)	0.012	
Bond angle (°)	1.563	
Average B-factor ($Å^2$)	34.0	
Total no. of atoms	2103	
Ramachandran plot		
Favoured (%)	90.3	
Additionally allowed (%)	9.3	
Generously allowed (%)	0.0	
Disallowed (%)	0.4	

Values within parenthesis represent corresponding to highest resolution shell.
[a] $R_{merge} = \sum_{hkl}\sum_{j=1}^{N}|I_{hkl} - I_{hkl}(j)| / \sum_{hkl}\sum_{j=1}^{N} I_{hkl}(j)$, where $I_{hkl}(j)$ is the j^{th} reflection of *hkl* plane.
[b] R factor $= (\Sigma_{hkl}||F_o(hkl)|-|F_c(hkl)||)/\Sigma_{hkl}|F_o(hkl)|$.
[c] R free is calculated for a random set of 5% of reflections not used in refinement.

to a constant temperature (298 K) and pressure (1 bar) by consecutive 100 ps MD simulations with NVT (constant volume and normal temperature) and NPT (constant normal pressure and normal temperature) ensembles. Production simulation of 10 ns was carried out with 2 fs time steps at constant temperature and pressure. Columbic and Van der waals' cut-off parameters were set to 10 Å.

3. Results and discussions

3.1. Overall structure of HadAB

HadAB was purified as tetramer (dimer of heterodimer) and crystallized in P432 space group with one heterodimer in the asymmetric unit. Initially for phasing molecular replacement (MR) method was attempted with various models of HadAB generated by using other prokaryotic and eukaryotic dehydratases/hydratases as template. But due to very low sequence homology MR was failed. Finally the phase information was obtained by Pb single isomorphous replacement with anomalous scattering (SIRAS) method at 2.7 Å resolution. The polypeptide backbone from residues 7 to144 of HadA and residue 2 to 142 of HadB can be traced in continuous electron density in the final model with R_{work}/R_{free} of 21.6/28.6.

The overall structure of HadAB heterodimer possesses two hot-dog (HD) folds each from a subunit. The HD fold is common to all FabA/FabZ enzymes and thioesterases [19,20]. The overall structure resembles a hot dog where the long α helices (sausage) are wrapped up by β sheets like 'bun'. HadA subunit consists of four α-helices (α1A–α4A) and six antiparallel β-strands (β1A–β6A), while HadB subunit consists of six α-helices (α1B–α6B) and six antiparallel β-strands (β1B–β6B). β-strands from both subunits are arranged like a wide antiparallel β sheet, which is covered by two long helices (α4A and α5B) from one side and therefore mimicking a double hot dog (DHD) fold (Fig. 1A and B). The structure can be seen as a DHD fold is split into two subunits. HadA and HadB heterodimer is stabilized via extensive hydrophobic contacts where almost 1388 $Å^2$ area from HadA and 1317 $Å^2$ area from HadB are involved (Supp. fig. 1). Helices α1A, α4A and strand β3A with α2B, α5B and β2B are associated in interface formation. Sequence structure analysis further shows that the N-terminal part of both α4A and α5B is populated with hydrophobic residues. Although hydrophobic interaction between β3A and β2B further reinforces the heterodimer stability, population of charged residues is higher in β3A (Asp88, Glu90, and Lys92). Side chains of these residues are exposed to the solvent protecting the core hydrophobic part of the interface. A sum total of 27 residues of HadA and 31 residues of HadB contribute to the heterodimeric interaction. Symmetry-mate analysis of HadAB corroborates to the tetrameric assembly of the enzyme in solution. Heterodimers from a particular pair of asymmetric unit builds up a tetramer assembly and are related by a two-fold symmetry (Fig. 1C). The inter-heterodimeric interface is built up by face-to-face interaction between α1A helices of HadA and α2B helices of HadB. Arg22, Lys24 and Arg26 of helix α1A of HadA are involved in salt-bridge interactions with Asp16 and Glu27 of α1A′ and vice versa whereas the interaction mediated via α2B helices are mostly hydrophobic with only exception of Asp43 participating in salt-bridge interaction with Asn95'.

3.2. Structural comparison and active site of HadAB

β-hydroxyacyl ACP dehydratases (DH) in the fatty acid biosynthesis pathway remove water molecule to form an unsaturated enoyl thioester [19,21]. Similar hot dog fold encompassing MaoC like hydratases (MaoCHs) performs the opposite reaction to convert unsaturated enoyl thioester to β-hydroxy thioester. DH and MaoCH catalyse the same reaction in opposite directions (dehydration/

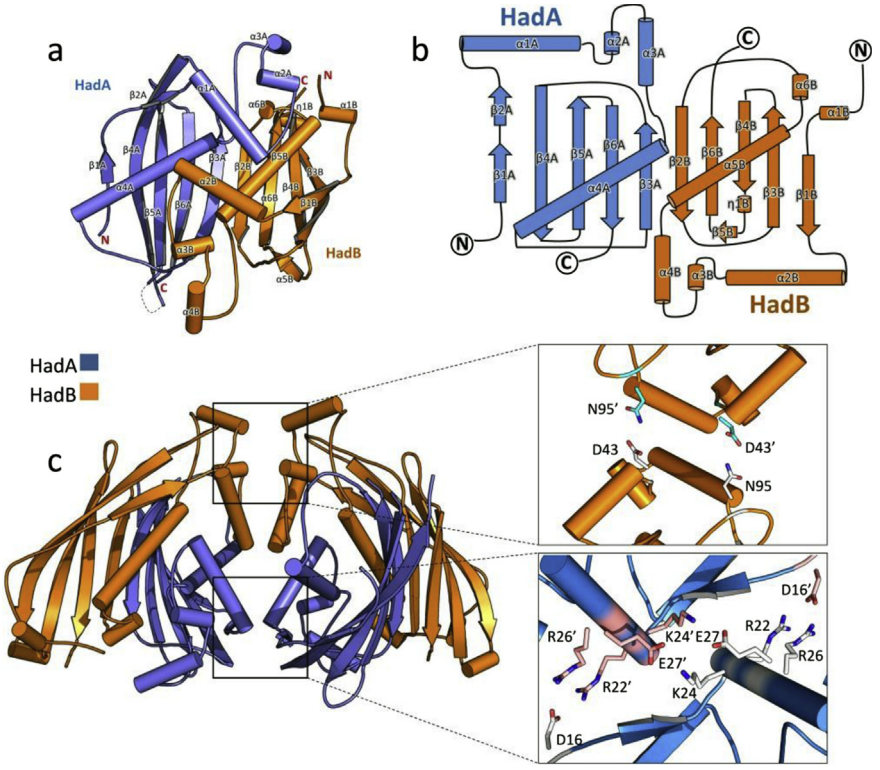

Fig. 1. Overall structure, topology and tetrameric assembly of HadAB: (a) Cartoon representation of HadA (slate) and HadB (orange) heterodimer. (b) Topology diagram of HadAB. (c) Tetrameric assembly of HadAB and the detailed salt-bridge interaction at the inter heterodimeric interface. The residues marked with 'represent symmetry mate. (For interpretation of the references to colour in this figure legend, the reader is referred to the web version of this article.)

hydration) following a similar acid-base mechanism [22], therefore, catalytic residues are essentially the same but the active site architecture become different. In homodimeric *Ec*FabA (PDB 1MKA), which has two active sites, His70 from one monomer and Asp84 from another monomer contribute to the active site. Hence two protomer of this conventional dehydratase equally participate to form two active sites. MaoCHs are generally involved in catabolic pathways or in polyhydroxyalkanoate (PHA) biosynthesis [23,24]. These hydratases are either monomer containing a single DHD fold and a single active site [25,26] or a homodimer containing DHD fold split into two protomers each containing an active site [27]. Recently, a similar DHD-fold-split MaoCH ChsH1-ChsH2 (PDB 4W78) with one active site structure has been determined that is involved in cholesterol catabolism in *M. tuberculosis* [28]. In all cases, the two catalytic residues of the active site in MaoCHs come either from a single protomer when it is HD homo/hetero dimer or from the C-terminal half when it is DHD monomer [25–28]. Here, the catalytic His and Asp are the part of a conserved motif "D-X-(N/Q)-X2-H-X-D-X3-A" called hydratase-2 motif [29,30]. Although HadAB entails DH reaction, both subunits share higher sequence homology with MaoCHs (STable 1). Sequence structure analysis of HadA and HadB separately shows that only HadB has the conserved hydratase-2 motif where Asp36 and His41 constitute the active site. The overhanging segment between α2B and α4B housing the catalytic residues is specific to all MaoCHs (Fig. 2A). Intriguingly, HadA and HadB shares weak sequence and structural homology (sequence identity 15% over 142 residues, r.m.s.d. 2.7 Å for 539 atoms) but HadA possesses similar overhanging segment (α1–α2–α3) lacking of hydratase-2 motif. Sequence alignment reveals that the catalytic residues in HadB are replaced with Asn34 and Phe39 respectively keeping Arg22, Ala29, and Ala45 as conserved residues in corresponding overhanging segment (Fig. 2B and C, SFig. 2). Hence, HadA is probably the inactive protomer of the HadAB complex acting as a scaffold for efficient catalysis of the long chain fatty acids. This hypothesis is in accordance with the fact that HadB can form heterodimer either with HadA or HadC participating in phase A and B of FAS-II pathway respectively [9]. Since phase A and phase B of FAS-II pathway deals with different chain lengths of the fatty acids, hence catalytic subunit HadB exchanges its structural counterpart commensurate with the length of fatty acyl chain. The fact is further justified from the biochemical assays showing that HadB alone is not catalytically competent (SFig. 3). Therefore HadAB is a novel single-active-site, DHD-fold-split, MaoC like dehydratase involved in fatty acid biosynthesis.

3.3. Substrate specificity of HadAB

DHs or MaoCHs deal with different chain lengths of the fatty acids but the key factor controlling the chain length specificity is elusive. A recent structure of a DHD-fold-split hydratase with single

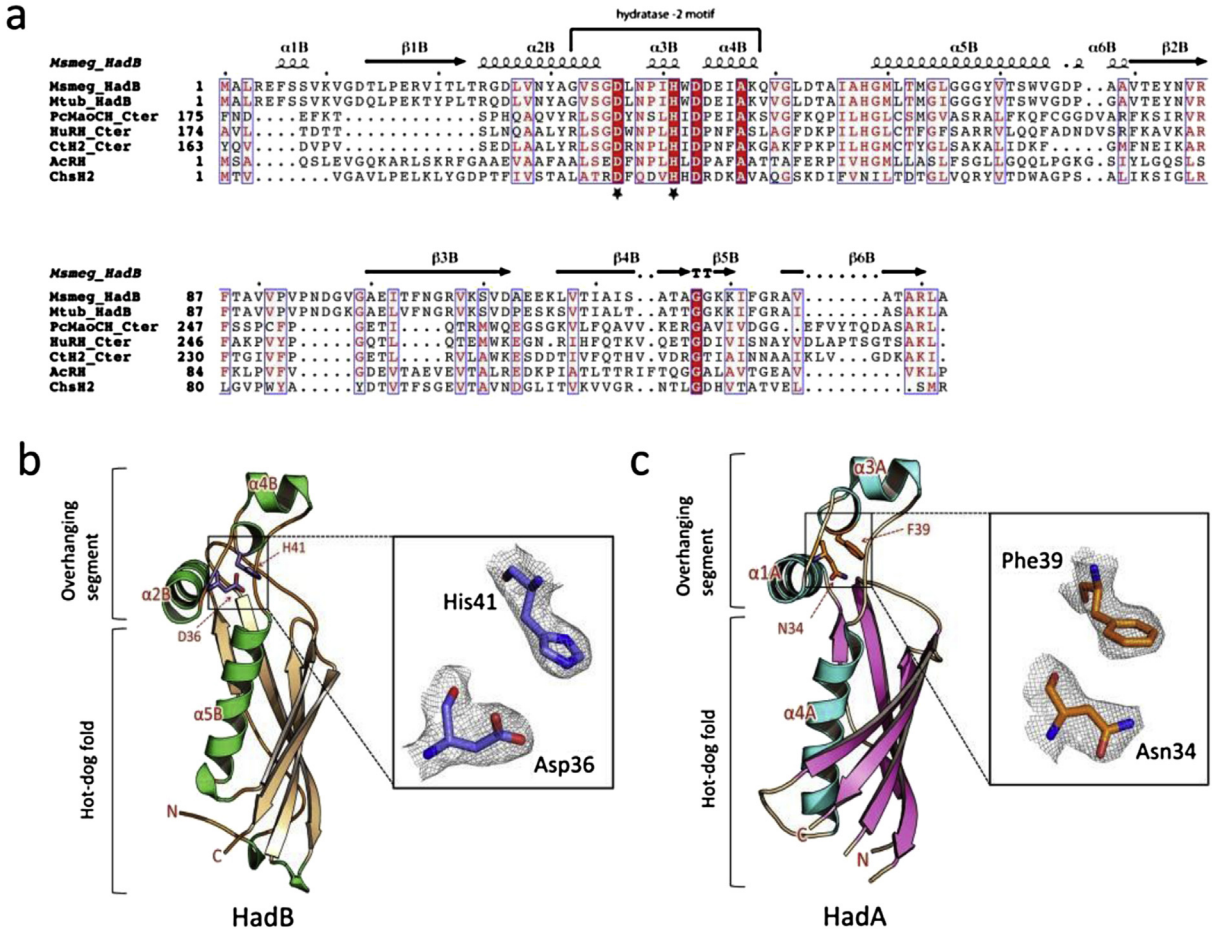

Fig. 2. Sequence-structure analysis of HadAB and the active site residues: (a) Structure-sequence alignment of HadB and MaoC hydratases: *M. smegmatis* HadB, *M. tuberculosis* HadB, C-terminal halves of: *P. capsisi* MaoCH (PcMaoCH), Human peroxisomal multifunctional enzyme 2-enoyl-CoA hydratase-2 (HuRH), *Candia tropicalis* hydratase-2 (CtH2), and *Aeromonas caviae* enoyl-CoA hydratase (AcRH) and *M. tuberculosis* ChsH2. The secondary structure elements of HadB are shown at the top of the alignment. The hydratase-2 motif in the overhanging segment is shown. Active site residues are indicated by Asterisk. (b, c) HadA and HadB are shown with corresponding overhanging segments. HadB catalytic residues (b) and the corresponding residues in the same position of HadA (c) are particularly shown in inset. 2Fo-Fc map is contoured at $\sigma = 1.6$.

active site, ChsH1-ChsH2 complex has shaded light on the mechanism [28]. Although HadAB and ChsH1-ChsH2 share poor sequence homology the structural homology is close (r.m.s.d C_α 1.7 Å for 1148 atoms). It was proposed that the longer the central α helix in hot-dog fold, the shorter the fatty acyl substrates is preferred (Fig. 3A). This proposition is in agreement with the existing structural and functional data but does not explain the substrate specificity of HadAB. Structural comparison indicates that the corresponding central α4A helix in HadAB is the longest (17 aa) among all known dehydratase structures, nevertheless the enzyme is specific for fatty acyl chain length C22 to C42 [9]. HadAB is then compared with AcRH (1IQ6), which also possesses a long α4 helix (16 aa) but is specific for shorter fatty acyl substrates [27]. Structural superposition indicates that the corresponding helix α4A in HadAB is nearly 20° slanted outward near the substrate entry side (Fig. 3A) and forming a much bigger space to accommodate a longer chain substrate. Also, the B factors of the corresponding helix segments in MaoCHs are usually higher (40–90 $Å^2$) and the secondary structure of this region is varying from protein to protein. MD simulation shows that although the overall of HadAB heterodimer is very stable (SFig. 4) the residue range 76–84 (peak at Arg79 with RMSF of 0.19 nm) pertaining to the α4A–β3A loop can exhibit conformational flexibility (Fig. 3B) so as to provide the room for the long chain fatty acyl substrates. Unlike HadA, HadC deals with longer fatty acyl chain in phase B of FAS-II. Sequence alignment reveals that there is a HadC specific insertion at the C-terminal possibly responsible for housing the longer acyl chain (SFig. 5).

3.4. Specificity of HadAB for CoA and/or ACP

MaoCHs are specific for coenzyme-A-linked substrates; on the contrary FabA/FabZ prefers ACP- based substrates. HadAB is structurally similar to MaoCHs but participates in an anabolic reaction like FabZ. So HadAB can be regarded as a link between two different kinds of dehydratases. Both CoA and ACP binding residues in HadAB are identified based on the corresponding substrate bound structures of MaoCH [24,28] and *E. coli* FabA-ACP complex [31]. The CoA bound structures of CtH2 (1PN4) and ChsH1–ChsH2 (4WNB) suggest an overall similar CoA binding mode in HadAB keeping a set of conserved interacting residues in all MaoCH (Fig. 3C). The CoA binding cavity in HadAB is situated between β3A and β2B of long β sheet at the interface of HadA and HadB. But the residues in adenine binding crater are not conserved in HadAB. Phe167 of ChsH1 and Arg79 of ChsH2 correspond to Phe758 and Arg855 of CtH2 respectively together involved in making the crater. These two residues are also conserved in other MaoCHs. In HadAB the Arg86 of HadA is similar but the Phe is substituted to Ala143 of HadA (Fig. 3C). The Phe to Ala substitution might have an effect of lowering the CoA specificity in HadAB. However, adenosine ribose 3′-phosphate group binding Arg113 from HadA and Arg86 from HadB are identified based on the structural superimpositions. Also it can be proposed that the backbone oxygen of Phe87 in HadB possibly be involved in hydrogen bonding interaction with adenine amino group and Arg113 might provide a stabilizing salt bridge interaction with 3′-phosphate group of ribose. Similarly the ACP–HadAB interaction is mapped based on the crystal structure of

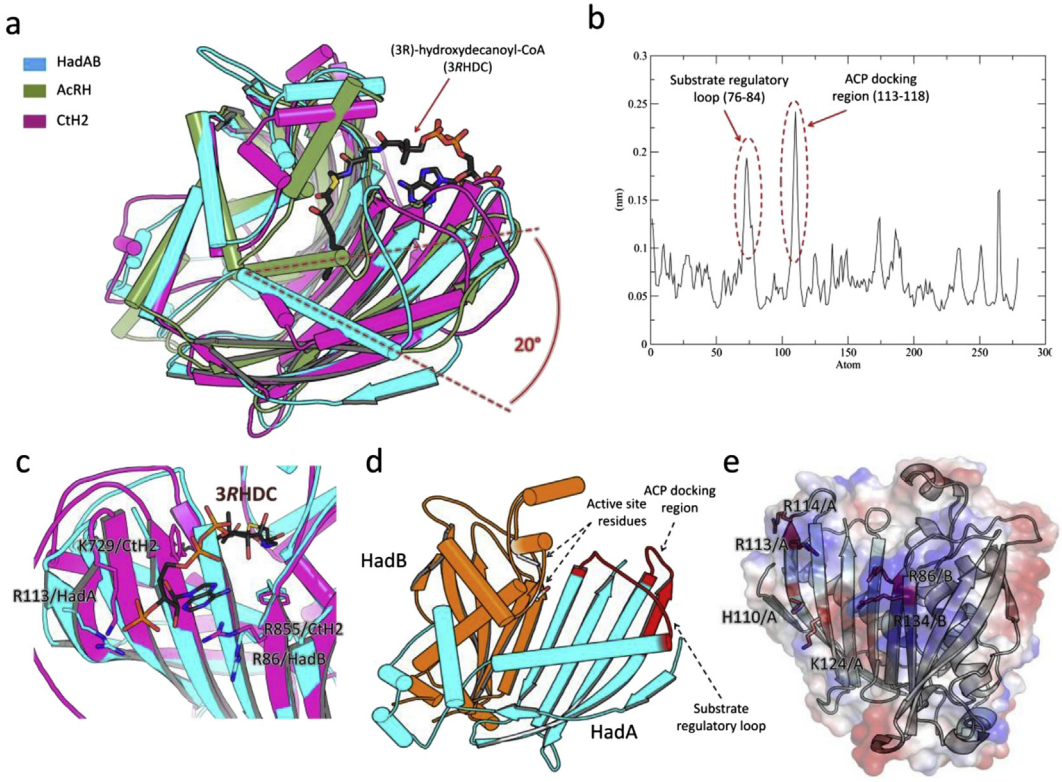

Fig. 3. Substrate specificity regulation and probable binding site: (a) Structural superposition of HadAB (cyan), AcRH monomer (smudge) and Ct-H2 (light magenta) are showing the variations in the scaffolding components of MaoCH, relative to substrate binding position. Structural comparison of the central hot-dog helices of HadA (17aa) and AcRH (16aa) implicating their relative orientations in substrate specificity. (b) The RMSF calculation during 10 ns MD simulations of HadAB complex. X- and Y- axis indicate the residue no and RMSF (nm) respectively. The graph is indicative to two specific flexible regions in HadAB complex. (c) The probable CoA and ACP binding site of HadAB. HadAB (cyan) and CtH2 (orange) are indicated. The residues interacting with 3*R*HDC are shown in stick. (b) The positively charged residues important for ACP docking are marked. The residues from HadA and HadB are represented by/A and/B respectively. (For interpretation of the references to colour in this figure legend, the reader is referred to the web version of this article.)

*Ec*FabA-ACP complex [31]. A positively charged cluster consisting of Arg113 and Arg114 from HadA and Arg86 of HadB is identified in proximity to the substrate entry channel (Fig. 3D and E). The conserved positioning of the positively charged residues for ACP docking and the neighbouring hydrophobic residues are proposed for dynamic interaction with helix II and helix III of ACP. Lys124 and His110 of HadA are indicated to initiate the salt bridge interaction with Helix II which follows the disruption of Helix III by Arg113 and Arg114 (Fig. 3E). This results in fatty acyl chain to come out from the interior of ACP. During the course of this process Ala111, Ala118, Ile120 and Val122 of HadA might stabilize the ACP helix II via hydrophobic interactions. Together these interactions probably allow the sequestered fatty acyl chain to come out from ACP hydrophobic core and protrude into the active site pocket of HadAB.

Conflict of interest

None.

Acknowledgment

We thank the Department of Biotechnology , Ministry of Science and Technology, Government of India (IIT/SRIC/BIO/LDO/2014-15/33 Dt. 17-04-2014) for financial assistance and for setting up the Macromolecular Crystallography housed at the Central Research Facility of the Indian Institute of Technology, Kharagpur (IITKGP), RB and DB thank to CSIR for an individual fellowship, AD and DH thanks to IITKGP the for an individual fellowship. We thank to Indian Institute of Technology, Kharagpur for funding project.

Appendix A. Supplementary data

Supplementary data related to this article can be found at http://dx.doi.org/10.1016/j.bbrc.2015.01.119.

Transparency document

The transparency document associated with this article can be found in the online version at http://dx.doi.org/10.1016/j.bbrc.2015.01.119.

References

[1] K. Takayama, C. Wang, G.S. Besra, Pathway to synthesis and processing of mycolic acids in Mycobacterium tuberculosis, Clin. Microbiol. Rev. 18 (2005) 81–101.
[2] L. Ciccarelli, S.R. Connell, M. Enderle, D.J. Mills, J. Vonck, M. Grininger, Structure and conformational variability of the mycobacterium tuberculosis fatty acid synthase multienzyme complex, Structure 21 (2013) 1251–1257.
[3] S.W. White, J. Zheng, Y.M. Zhang, Rock, the structural biology of type II fatty acid biosynthesis, Annu. Rev. Biochem. 74 (2005) 791–831.
[4] R.J. Heath, C.O. Rock, Roles of the FabA and FabZ β-hydroxyacyl-acyl carrier protein dehydratases in *Escherichia coli* fatty acid biosynthesis, J. Biol. Chem. 271 (1996) 27795–27801.
[5] A. Gurvitz, J.K. Hiltunen, A.J. Kastaniotis, Heterologous expression of mycobacterial proteins in *Saccharomyces cerevisiae* reveals two physiologically functional 3-Hydroxyacyl-Thioester dehydratases, HtdX and HtdY, in addition to HadABC and HtdZ, J. Bacteriol. 191 (2009) 2683–2690.
[6] E. Sacco, N. Slama, K. Bäckbro, T. Parish, F. Laval, M. Daffé, N. Eynard, A. Quémard, Revisiting the assignment of Rv0241c to fatty acid synthase type II of *Mycobacterium tuberculosis*, J. Bacteriol. 192 (2010) 4037–4044.
[7] R. Biswas, D. Dutta, A.K. Das, Cloning, overexpression, purification, crystallization and preliminary X-ray diffraction analysis of Rv0241c (HtdX) from Mycobacterium tuberculosis H37Rv, Acta Cryst. F. 69 (2013) 1110–1113.
[8] D. Dutta, S. Bhattacharyya, A. Roychowdhury, R. Biswas, A.K. Das, Crystal structure of Hexanoyl-CoA bound to β-ketoacyl reductase FabG4 of *Mycobacterium tuberculosis*, Biochem. J. 450 (2013) 127–139.
[9] E. Sacco, A.S. Covarrubias, H.M. O'Hare, P. Carroll, N. Eynard, T.A. Jones, T. Parish, M. Daffé, K. Bäckbro, A. Quémard, The missing piece of the type II fatty acid synthase system from *Mycobacterium tuberculosis*, Proc. Natl. Acad. Sci. 104 (2007) 14628–14633.
[10] N. Slama, J. Leiba, N. Eynard, M. Daffé, L. Kremer, A. Quémard, V. Molle, Negative regulation by Ser/Thr phosphorylation of HadAB and HadBC dehydratases from Mycobacterium tuberculosis type II fatty acid synthase system, Biochem. Biophys. Res. Commun. 412 (2011) 401–406.
[11] W. Kabsch, Automatic processing of rotation diffraction data from crystals of initially unknown symmetry and cell constants, J. Appl. Cryst. 26 (1993) 795–800.
[12] G. Sheldrick, A short history of SHELX, Acta Crystallogr. Sect. A: found, Crystallogr 64 (2008) 112–122.
[13] C. Vonrhein, E. Blanc, P. Roversi, G. Bricogne, Automated structure solution with autoSHARP, Methods Mol. Biol. 364 (2007) 215–230.
[14] K. Cowtan, The Buccaneer software for automated model building. 1. Tracing protein chains, Acta Cryst. D. 62 (2006) 1002–1011.
[15] P. Emsley, K. Cowtan, Coot: model-building tools for molecular graphics, Acta Cryst. D. 60 (2004) 2126–2132.
[16] G.N. Murshudov, A.A. Vagin, E.J. Dodson, Refinement of macromolecular structures by the maximum-likelihood method, Acta Cryst. D. 53 (1997) 240–255.
[17] S. Pronk, S. Páll, R. Schulz, P. Larsson, P. Bjelkmar, R. Apostolov, M.R. Shirts, J.C. Smith, P.M. Kasson, D. Spoel, B. Hess, E. Lindahl, GROMACS 4.5: a high-throughput and highly parallel open source molecular simulation toolkit, Bioinformatics 29 (2013) 845–854.
[18] G.A. Kaminski, R.A. Friesner, Evaluation and reparametrization of the OPLS-AA force field for proteins via comparison with accurate quantum Chemical calculations on peptides, J. Phys. Chem. B 105 (2001) 6474–6487.
[19] M. Leesong, B.S. Henderson, J.R. Gillig, J.M. Schwab, J.L. Smith, Structure of a dehydratase-isomerase from the bacterial pathway for biosynthesis of unsaturated fatty acids: two catalytic activities in one active site, Structure 4 (1996) 253–264.
[20] M.S. Kimber, F. Martin, Y. Lu, S. Houston, M. Vedadi, A. Dharamsi, K.M. Fiebig, M. Schmid, C.O. Rock, The structure of (3R)-hydroxyacyl-acyl carrier protein dehydratase (FabZ) from *Pseudomonas aeruginosa*, J. Biol. Chem. 279 (2004) 52593–52602.
[21] L. Moynié, S.M. Leckie, S.A. McMahon, F.G. Duthie, A. Koehnke, J.W. Taylor, M.S. Alphey, R. Brenk, A.D. Smith, J.H. Naismith, Structural insights into the mechanism and inhibition of the β-hydroxydecanoyl-acyl carrier protein dehydratase from *Pseudomonas aeruginosa*, J. Mol. Biol. 425 (2013) 365–377.
[22] J.W. Labonte, C.A. Townsend, Active site comparisons and catalytic mechanisms of the hot dog superfamily, Chem. Rev. 113 (2013) 2182–2204.
[23] T. Fukui, N. Shiomi, Y. Doi, Expression and characterization of (R)-specific enoyl coenzyme A hydratase involved in polyhydroxyalkanoate biosynthesis by Aeromonas caviae, J. Bacteriol. 180 (1998) 667–673.
[24] K.M. Koski, A.M. Haapalainen, J.K. Hiltunen, T. Glumoff, A two domain structure of one subunit explains unique features of eukaryotic hydratase 2, J. Biol. Chem. 279 (2004) 24666–24672.
[25] K.M. Koski, A.M. Haapalainen, J.K. Hiltunen, T. Glumoff, Crystal structure of 2-enoyl-CoA hydratase 2 from human peroxisomal multifunctional enzyme type 2, J. Mol. Biol. 345 (2005) 1157–1169.
[26] H. Wang, K. Zhang, J. Zhu, W. Song, L. Zhao, X. Zhang, Structure reveals regulatory mechanisms of a MaoC-like hydratase from Phytophthora capsici involved in biosynthesis of polyhydroxyalkanoates (PHAs), PLoS One 8 (2013) e80024.
[27] T. Hisano, T. Tsuge, T. Fukui, T. Iwata, K. Miki, Y. Doi, Crystal structure of the (R)-specific enoyl-CoA hydratase from *Aeromonas caviae* involved in polyhydroxyalkanoate biosynthesis, J. Biol. Chem. 278 (2003) 617–624.
[28] M. Yang, K.E. Guja, S.T. Thomas, M. Garcia-Diaz, N.S. Sampson, A distinct MaoC-like Enoyl-CoA hydratase architecture mediates cholesterol catabolism in *Mycobacterium tuberculosis*, ACS Chem. Biol. 9 (2014) 2632–2645.
[29] S.C. Dillon, A. Bateman, The hotdog fold: wrapping up a superfamily of thioesterases and dehydratases, BMC Bioinforma. 5 (2004) 109.
[30] L.S. Pidugu, K. Maity, K. Ramaswamy, N. Surolia, K. Suguna, Analysis of proteins with the "hot dog" fold: prediction of function and identification of catalytic residues of hypothetical proteins, BMC Struct. Biol. 9 (2009) 1–16.
[31] C. Nguyen, R.W. Haushalter, D.J. Lee, P.R. Markwick, J. Bruegger, G. Caldara-Festin, K. Finzel, D.R. Jackson, F. Ishikawa, B. O'Dowd, J.A. McCammon, S.J. Opella, S.C. Tsai, M.D. Burkart, Trapping the dynamic acyl carrier protein in fatty acid biosynthesis, Nature 505 (2014) 427–431.